ORGANIC PROCESS RESEARCH & DEVELOPMENT
OPR&D

pubs.acs.org/OPRD Article

On-Demand Continuous Manufacturing of Ciprofloxacin in Portable Plug-and-Play Factories: Development of a Highly Efficient Synthesis for Ciprofloxacin

Cameron Armstrong, Yuma Miyai, Anna Formosa, Dale Thomas, Esther Chen, Travis Hart, Victor Schultz, Bimbisar K. Desai, Angela Y. Cai, Alexandra Almasy, Klavs Jensen, Luke Rogers,* and Tom Roper*

Cite This: *Org. Process Res. Dev.* 2021, 25, 1524−1533 Read Online

ACCESS | Metrics & More | Article Recommendations | Supporting Information

ABSTRACT: The experimental approach taken and challenges overcome in developing a high-purity production (>100 g) scale process for the telescoped synthesis of the antibiotic ciprofloxacin is outlined. The process was first optimized for each step sequentially with regard to purity and yield, with necessary process changes identified and implemented before scaling for longer runs. These changes included implementing a continuous liquid−liquid extraction (CLLE) step and eliminating and replacing the base 1,8-diazabicyclo[5.4.0]undec-7-ene (DBU) initially used in the ring-closure step due to DBU plausibly forming a decomposition side product that negatively impacted the final product purity. Process conditions were scaled 1.5−2-fold in order to enable the ultimate project goal of producing enough crude ciprofloxacin within 24 h to manufacture 1000 250 mg tablets. Working toward this goal, several production-scale runs were carried out to assess the reproducibility and robustness of the finalized process conditions, with the first three steps being run continuously up to 22 h and the last two steps being run continuously up to 10 h. The end result is a process with a throughput of ∼29 g/h (∼700 g/24 h) with a crude product stream profile of 94 ± 2% and 34 ± 3 mg/mL after five chemical transformations across four reactors and one continuous CLLE unit operation with each intermediate step maintaining a purity >95% by HPLC.

KEYWORDS: *continuous pharmaceutical manufacturing, design of experiments, flow chemistry, continuous liquid−liquid extraction*

INTRODUCTION

The paradigm of continuous manufacturing (CM) in the pharmaceutical sector is no longer a novel concept. The research and development efforts of industries and academia have shown an increasing trend toward the adaptation of CM in processes where there is a balance between the benefits and practicality of implementation.[1−7] With regard to the active pharmaceutical ingredient (API) synthesis, implementation of CM has been encouraged by the Food and Drug Administration (FDA);[8,9] however, in practice, it has typically been relegated to cases where there is a direct incentive to depart from the historical batch process, coming from the possible mitigation of existing process safety risks or acute problems with manufacturability.[4,10]

For low-volume drugs and medicines which require immediate production and distribution on short notice, such as during pandemics or shortages, distributed CM provides a potential method for on-demand and local production of critical medicines. This concept led to the development of the Pharmacy-on-Demand platform which was originally envisioned to improve access to life-saving medications on the battlefield.[11,12] The overarching concept is that miniaturized manufacturing platforms can be modularized to produce urgently needed APIs from key starting materials and that these modules can be strategically located for rapid localized distribution of life-saving medicines. As a proof of concept, a campaign to test the capabilities of such a platform was carried out, where quantities of several APIs were produced within a short window of time.[13−15] However, beyond proving the idea possible, there was a challenge of developing a process capable of producing API with high enough quality and reproducibility to be registered with the FDA and manufactured for human use.

The current work addresses the purity, yield, and reproducibility for a single drug—the antibiotic ciprofloxacin, which is listed by the World Health Organization as an essential medicine,[16] with the ultimate goal of filing an abbreviated new drug application (ANDA) with the FDA. Ciprofloxacin additionally was selected as the target molecule because the chemistry is typical of most small molecules and to prove robustness of the drug product manufacturing unit by taking on the challenge of the high-dosage form (250 mg tid). Specifically, this work focuses on transforming an existing process with suboptimal purity, throughput, and reproducibility into an efficient process that affords a product with high purity and which both is reproducible and has an adequate throughput for commercialization. The process was scaled to enable the ultimate future goal

Received: April 3, 2021
Published: June 25, 2021

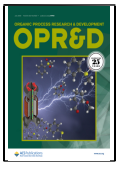

https://doi.org/10.1021/acs.oprd.1c00118
Org. Process Res. Dev. 2021, 25, 1524−1533

Scheme 1. Initial Telescoped Continuous Synthesis for Ciprofloxacin (Reproduced with Permission From ref 17. Copyright 2017 Angewandte Chemie International Edition, John Wiley and Sons)

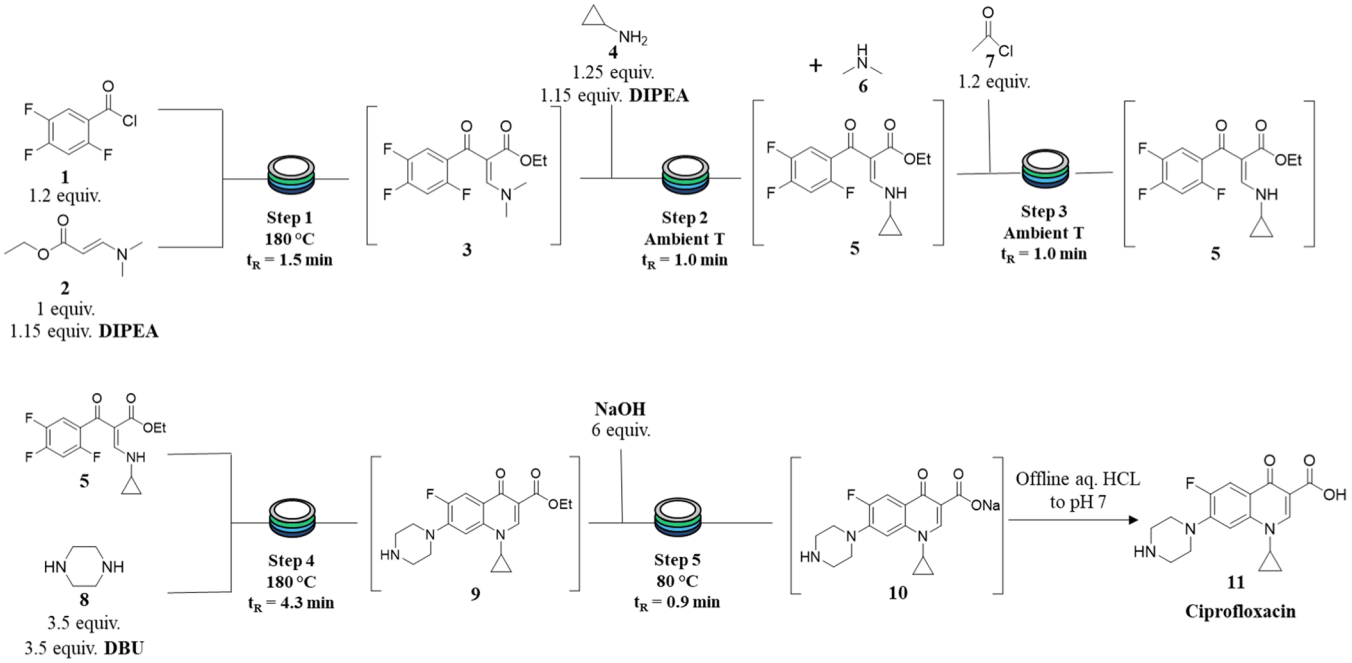

Scheme 2. Updated Continuous Process for Ciprofloxacin as Developed at MIT

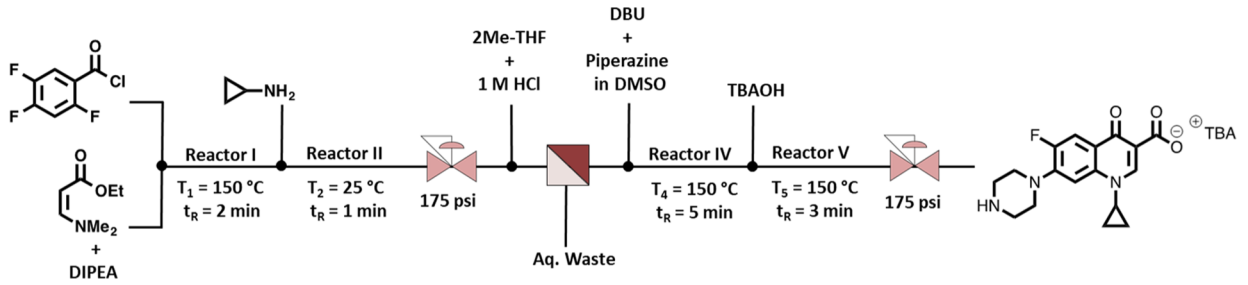

of continuously producing 1000 tablets within a 24 h window, which is considered a reasonable throughput for a decentralized network of manufacturing sites.

The starting point for this process was the telescoped flow synthesis for the ciprofloxacin sodium salt **10** published by Lin et al. in 2017 (Scheme 1)[17] which involves five steps carried out in tubular reactors, with acetyl chloride **7** infused into the step 2 stream to remove the byproduct dimethylamine (DMA) **6** by way of an acylation reaction. Subsequent offline acidification and filtration steps afforded ciprofloxacin **11** and ciprofloxacin hydrochloride (not shown) with an overall yield of 60% across eight total steps. Several areas were identified for development to ensure that the process could reproducibly and reliably produce ciprofloxacin in sufficient quantity and quality. The four major areas identified are listed below:

1 determine optimized operating and stoichiometric parameters for each step in order to minimize impurity formation and increase product yield,

2 implement a continuous liquid−liquid extraction (CLLE) for removal of DMA **6**, thus eliminating the use of acetyl chloride as a sequestering agent,

3 investigate and eliminate the driving forces for solid formation and impurity formation in the final two steps to avoid blockages in the reactors and provide an extremely high level of in-solution product purity, and

4 establish the robustness of the improved process by performing several end-to-end continuous runs with durations between 12 and 24 h.

Further development of the Lin process for ciprofloxacin was carried out initially at Massachusetts Institute of Technology (MIT) as described in the aforementioned proof-of-concept CM campaigns along with the other API targets in this project.[13−15] The major process adaptations from this initial development involved substituting the acetyl chloride **7** infusion with a CLLE operation and the substitution of NaOH with TBAOH in the hydrolysis step. The crude ciprofloxacin material generated from that campaign at MIT is what is referenced in the complementary paper of this series on the purification modules, and this synthesis process is depicted in Scheme 2.[18] However, while this process was more refined than the initial telescoped synthesis, more work was required in order to enable the process to run smoothly for long durations, while maintaining a high degree of product purity throughout the continuous API production. This development work, and the accompanying successful long runs, was carried out at Virginia Commonwealth University (VCU) and is the focus of this paper.

https://doi.org/10.1021/acs.oprd.1c00118
Org. Process Res. Dev. 2021, 25, 1524−1533

Table 1. Continuous Flow DOE Results for Steps 1−2 Holding Step 2 Variables Constant

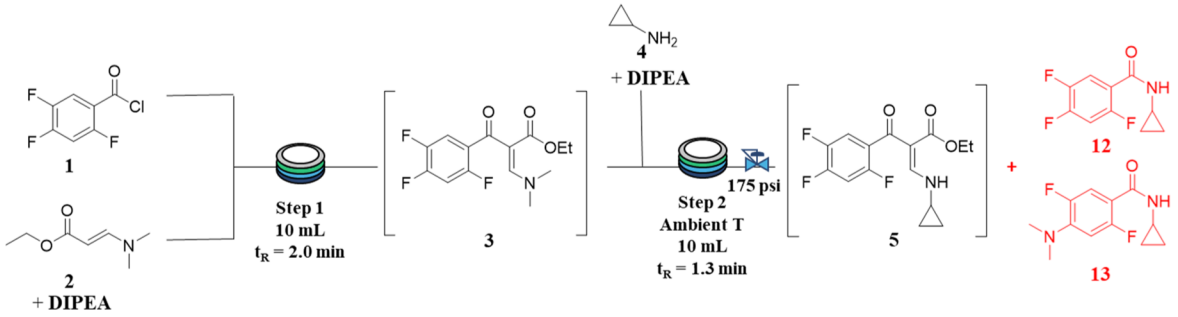

run	step 1 temperature (°C)	1 feed concentration	1 feed concentration	LCAP of 5 (%)*	5 yield (%)	LCAP of 12 (%)*	LCAP of 13 (%)*
1	180	1.6	1.34	82.24	92.9	2.5	5.68
2	140	0.95	1.34	95.3	100.4	0.8	0.13
3	180	0.95	1.34	95.3	85.3	0.2	0.36
4	160	1.275	1.17	91.9	91.5	1.5	1.70
5	180	1.6	1	30.0	51.3	13.6	24.35
6	180	0.95	1	94.1	89.0	0.8	0.37
7	140	1.6	1	31.6	49.8	12.6	26.12
8	140	0.95	1	94.4	84.5	1.7	0.16
9	140	1.6	1.34	85.2	93.0	6.3	2.16
10	160	1.275	1.17	92.8	90.6	2.4	0.38

The DIPEA equivalents with respect to **2** and **4** were held constant at 1.25. The **4** concentration was held constant at 1.25 M. All starting material feed streams ran at 2.5 mL/min. Residence times recorded are V/Q values. * designates average of duplicate HPLC samples.

Table 2. Continuous Flow DOE Results for Steps 1−2 Holding Step 1 Variables Constant

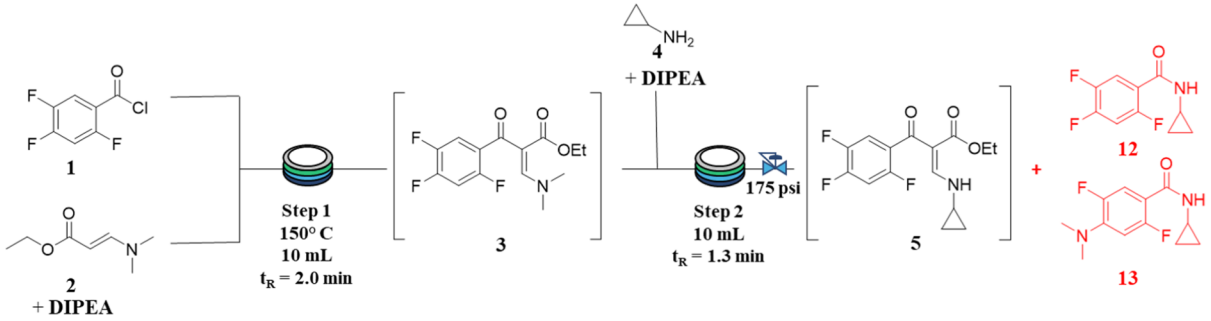

run	step 1 temperature (°C)	4 feed concentration	DIPEA equivalents to 4 (−)	LCAP of 5 (%)*	5 yield (%)	LCAP of 12 (%)*	LCAP of 13 (%)*
1	45	1.25	0.575	95.35	92.0	0.84	0.31
2	25	1.5	0	94.35	94.4	1.84	0.07
3	25	1	0	94.06	93.6	1.04	1.13
4	65	1.5	1.15	95.47	93.3	0.86	0.13
5	65	1	1.15	93.73	93.1	0.84	1.33
6	65	1	0	93.82	93.1	0.92	1.53
7	25	1.5	1.15	95.09	94.2	1.01	0.1
8	45	1.25	0.575	95.16	91.9	0.87	0.27
9	25	1	1.15	93.60	92.2	1.01	1.13
10	65	1.5	0	94.40	95.6	1.71	0.08

All step 1 conditions were held constant. The DIPEA equivalents with respect to **2** were held constant at 1.15. All starting material feed streams ran at 2.5 mL/min. Residence times recorded are V/Q values. Runs at ambient temperature are assumed to be 25 °C. * designates average of duplicate HPLC samples.

METHODS AND MATERIALS

Materials. All starting materials were used as received from vendors. 2,4,5-Tri-fluorobenzoyl chloride (98%) was procured from Oakwood Chemical (Estill, SC). Ethyl 3-(dimethylamino)acrylate (99%) was procured from TCI America (Portland, OR). 1 M hydrochloric acid was procured from Midland Scientific (Omaha, NE). Acetonitrile (99.8%), cyclopropylamine (98%), *N,N*-diisopropylethylamine (DIPEA) (>99%), 2-methyltetrahydrofuran (>99.5%), piperazine (99%), 1,8-diazabicyclo[5.4.0]undec-7-ene (DBU) (98%), tetrabutylammonium hydroxide (40 wt % in H_2O), and dimethyl sulfoxide (>99%) were all procured from Sigma-Aldrich (St. Louis, MO).

Experimental Apparatus. All flow synthesis experiments were performed using either a thick-walled perfluoroalkoxy (PFA) tubing (1/16″ i.d., 1/8″ o.d.) in a bath of heated silicone

https://doi.org/10.1021/acs.oprd.1c00118
Org. Process Res. Dev. 2021, 25, 1524−1533

oil or a thin-walled PFA tubing (1/16″ or 0.106″ i.d., 1/8″ o.d.) enclosed in aluminum clamshell reactor plates. Size 1/4−28 nuts, tee-junctions, and unions all made of poly-ether-etherketone (PEEK) were used for assembling the tubing components of the reactors and feed lines (IDEX Health & Science, Lake Forest, IL). Back pressure regulators (Model BPR-10) from Zaiput Flow Technologies (Waltham, MA) were applied at the outlets of step 2 and step 5 (175 psi each). An assortment of either Milligat (Global FIA; Fox Island, WA) or Eldex (Napa, CA) pumps were applied to pump reagents for all experiments. For the continuous extraction, the final version for the gravity separation unit was a custom 100 mL glass vessel manufactured by Ace Glass Inc. (Vineland, NJ).

Analytical Procedure. Reaction stream samples were collected after approximately five residence times for each experiment and diluted in a mixture of acetonitrile and aqueous buffer as further described in the Supporting Information (SI). Samples were then analyzed via high-performance liquid chromatography (HPLC) with ultraviolet detection as described in the Supporting Information, with additional analysis carried out using liquid chromatography−mass spectrometry (LCMS) also as described in the Supporting Information Starting material stability for the stocks of acyl chloride **1**, acrylate **2**, cyclopropylamine **4**, and piperazine **8** was performed with gas chromatography (GC) as described and depicted in the Supporting Information.

The process analytical technology (PAT) was applied in two locations; an in-line infrared spectrometer equipped with a fiber-optic probe was used after reaction step 2 to monitor intermediate and product peaks (Mettler-Toledo, Columbus, OH), and an in-line Raman spectrometer equipped with a flow cell was applied to monitor the final outlet product stream (Marqmetrix, Seattle, WA). An in-depth overview of the PAT data and strategy is beyond the scope of this article, but as a vital component of the project, a separate article is being prepared with further analysis.

Software. All data from Design of Experiment (DOE) studies were analyzed using the software JMP 15 (SAS Institute, Cary, NC). Milligat pumps and temperature control for the clamshell reactors were controlled via LabVIEW process control architectures (National Instruments, Austin, TX).

RESULTS AND DISCUSSION

Steps 1 and 2. Step 1 in this synthesis is an acylation to produce keto-ester **3**, followed by a rapid amine substitution (step 2), providing cyclopropyl-enamine **5**. Due to the high reactivity of **3** and the rapid nature of step 2, these first two steps were carried out without analysis of intermediate **3** after step 1, assuming that any perturbations to the process caused by changes to either step would be captured by analyzing the step 2 outlet stream. Two DOE[19,20] studies were performed for these synthesis steps: the first focused on step 1 variables, holding step 2 variables constant (Table 1), and the second focused on step 2 variables, holding constant the previously optimized step 1 conditions (Table 2).

A potential source of impurities were side reactions between reaction intermediates and excess acyl chloride **1**, cyclopropyl-amine **4**, or the DMA **6** species displaced from **3** in step 2. To test this, the study was designed so that **1** was the limiting reagent for several of the runs (Table 1; runs 2, 3, 6, and 8). The study results with respect to purity of **5**, represented as area percent by liquid chromatography (LCAP), indicated that ensuring that using acyl chloride **1** as the limiting reagent significantly increased the LCAP (Table 1; runs 2, 3, 6, and 8). The proposed impurity species **12** and **13** were also observed to be sensitive to relative quantities of **1** in the stream as their LCAP levels were significantly increased when equivalents of **1** to **2** were 1.6:1 (Table 1; runs 5 and 7), whereas when **2** was in excess, species **12** and **13** were observed at their lowest LCAP values (Table 1; runs 2, 3, 6, and 8). Effects on purity, conversion, and impurity formation with regard to the step 1 reactor temperature were essentially negligible compared to effects of varying concentrations and equivalents of **1** and **2**. Further experiments isolating temperature as a variable confirmed that an intermediate temperature was observed to maximize the purity and yield of **5** (see the Supporting Information). For the second DOE study described below, the selected conditions for step 1 were **2** at 1.2 M with 1.25 equiv of DIPEA (with respect to **2**) and **1** at 1.0 M, carried out at 150 °C for 2 min.

The second study, which focused on step 2 (Table 2), showed considerably less variation in LCAP and yield of **5** across experiments when compared to step 1, with no significant difference observed between runs. Some degree of variation was expected when the concentration of **4** was reduced to 1 M, effectively becoming equimolar with regard to the theoretical step 1 outlet concentration of enamine **3**, and an observed significant effect was that species **13** was observed to have LCAP values >1.0% at this set point (Table 2; runs 3, 5, 6, and 9). With **4** at 1.5 M, levels of **13** were substantially reduced to ∼0.1%; however, species **12** was seen to increase in some cases (Table 2; runs 2 and 10). The presumption that the reaction was rapid enough to perform at room temperature was verified as no clear trend with temperature was observed going from ambient conditions to 65 °C. This short time frame additionally indicated future potential for reactor volume reduction to decrease overall system residence time and plausibly reduce time for further side reactions to occur. Furthermore, the effect of DIPEA was determined to be negligible and was therefore removed as a reagent from step 2.

Based off these studies and various one-factor validation experiments, the step 1 optimized conditions are 1.2 M of **2** with 1.15 equiv of DIPEA (with respect to **2**) and 1.0 M of **1** heated at 150 °C for 2 min. For step 2, the conditions selected are 1.25 M of **4** with no additional DIPEA at ambient temperature for 1.3 min. These conditions ultimately offered a purity by LCAP for **5** of 95 ± 1% and an overall yield of 91 ± 2% across two chemical transformations in two reactors, with a **5** stream concentration of 95 ± 3 mg/mL.

Development of CLLE for Step 3. In the original process, the DMA **6** byproduct was removed by reaction with acetyl chloride **7** as depicted above in Scheme 1. However, this procedure carried forward the resulting *N*,*N*-dimethylacetamide (not shown) through the process and further diluted the process stream. Additionally, acetonitrile was used as the solvent for steps 1−2 but is not a favorable solvent for the remaining two steps due to solubility concerns with the intermediates formed therein. The process enhancement implemented was a CLLE unit operation (Figure 1) that performed three essential tasks: (1) adequate removal of DMA **6** and other aqueous impurities, (2) increasing the concentration of the reaction intermediate **5** in the organic stream, and (3) a solvent exchange to 2-methyltetrahydrofuran (2-MeTHF) which is believed to be a more suitable solvent for the subsequent reactions.

Various designs for the CLLE unit operation were considered including a continuous membrane separation;[21] however, the

https://doi.org/10.1021/acs.oprd.1c00118
Org. Process Res. Dev. 2021, 25, 1524−1533

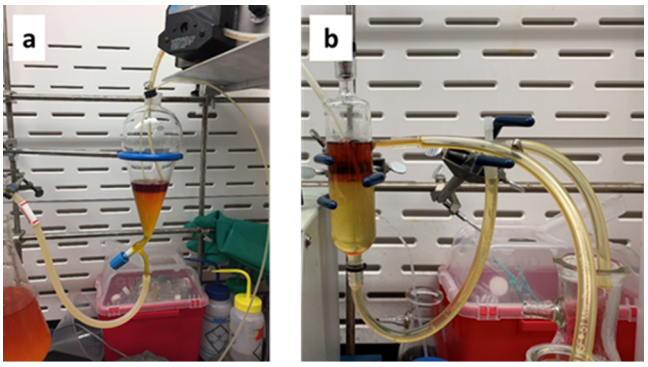

Figure 1. Two iterations of the gravity separator: a gravity separator using a standard laboratory separatory funnel with pumping out of the organic layer into a surge vessel (a) and a custom gravity separator with an organic overflow egress to a surge vessel (b).

only solvent systems observed to extract effectively with the membrane for this system were chlorinated solvents. These solvents did not align with the desired green chemistry principles and thus were not considered further.[22] A gravity separation approach was tested and ultimately selected for the process. The selected solvent system was 1 M HCl for the aqueous phase and 2-MeTHF for the organic phase, in a 5:2:3 (aqueous:organic:-reaction stream) volumetric ratio with respect to the step 2 outlet stream containing **5**. This solvent ratio was selected due to displaying a rapid settling time (<1 min) of the two phases, a high organic layer purity of **5**, and providing the necessary concentration of **5** to be taken directly as the feed for step 4 (Table 3). Additionally, it is desirable to maintain an adequate organic layer volume with respect to the aqueous layer volume so as to enable drawing off the organic phase without risking aqueous phase collection (Table 3). The gravity separation system is particularly amenable to a continuous system by maintaining control over the height of the phase interface and the organic phase level by setting the tee-piece height for the aqueous outflow or otherwise controlling the aqueous outflow.[10,23] Additionally, the application of an overflow outlet made the use of an additional pump for the organic phase out of the separator obsolete, simplifying the process equipment requirements (Figure 1). The residence time of the extraction unit operation was estimated as steady-state fill volume of the extraction vessel (75 mL) divided by the combined flow rate into the vessel. This fill volume was observed to be constant for subsequent volumetric flow rate scale-ups, yielding a residence time of 3 min for the unscaled process and 2 min for the scaled process. The organic stream of the continuous separation was consistently >95% by HPLC and 126 ± 2 mg/mL of **5** (equating to an extraction efficiency of 88 ± 2%), as shown below in the long-run data of Table 6.

Steps 4 and 5. A major concern in the optimization of steps 4 and 5 was the formation of an insoluble intermediate, believed to be the transient quinolone precursor **14** of cipro-ester **9**, and on multiple occasions in the initial development work, there were reactor failures caused by partial and/or total blockage of the step 4 reactor lines. One driving force of these phenomena was the use of NaOH to produce the ciprofloxacin sodium salt. As such, investigations into avoiding this step were made, and efforts were taken to perform the hydrolysis of intermediate **9** by means of the addition of a non-nucleophilic base in step 5. Because of the lingering possibility of a solubility issue, steps 4–5 were optimized concurrently to avoid solids forming either in the reactor or in the collection vessel with a standalone step 4 setup. Another process challenge was the high sensitivity of the product stream quality to reagent equivalents due to there being three distinct chemical transformations occurring over two reactors along with multiple competing side reactions. Therefore, before studying effects of reagent equivalents in flow, an initial study to map out the effects of the temperature set points of each reactor and residence time of step 4 was carried out.

In order to assess process stability and ensure the steady state, each set of conditions was run continuously for approximately 1 h (~five system residence times) before sample collection. The conditions were then adjusted to the next set of conditions for an uninterrupted study time of approximately 12 h in flow. The study revealed that increases in the temperature and residence time of step 4 significantly affected the product stream purity of **11**. The comparison of runs 3 versus 10 as well as runs 4 versus 5 in Table 4 emphasizes this finding. Additionally, the side-reaction product **15** was observed to be at its highest LCAP levels when the step 4 temperature was at 180 °C, and when at 180 °C, a relative increase in **15** was observed when increasing the step 4 residence time from 5 to 7 min, suggesting a synergistic effect of step 4 residence time and temperature on this impurity species (Table 4; runs 1, 5, 8, and 10). A lack of trends in both the quantities of the unhydrolyzed intermediate **9** or hydrolyzed product **11** indicated that the temperature of step 5 had a negligible effect on the hydrolysis reaction across the

Table 3. Volumetric Ratio Screening for Extraction of 5 in Step 3

run	1 M HCL vol. ratio (−)	5 vol. ratio (−)	2-Me THF vol. ratio (−)	LCAP of 5 in org. layer (%)	LCAP of 5 in aq. layer (%)	conc. of 5 in org. layer (mg/mL)	conc. of 5 in aq. layer (mg/mL)	settling time (s)	org. layer volume (mL)	aq. layer volume
1	5	3	2	85.8	61.4	112.5	10.4	47	3.7	15.3
2	5	1	2	82.9	23.9	61.7	2.1	36	1.9	17.5
3	5	3	1	88.4	69.4	226.8	27.1	156	2.9	16.8
4	1	1	1	78.7	68.1	51.6	15.4	38	11.2	8.5
5	2	1	1	85.0	64.3	137.4	16.5	34	5.1	14.4
6	3	2	1	86.9	62.9	228.4	17.1	37	3.8	15.5
7	3	1	2	71.7	32.0	77.3	3.9	41	5.9	13.3
8	2	3	1	80.1	66.2	156.8	30.5	48	9.3	10.0
9	2	1	2	80.4	31.4	65.5	4.2	75	9.5	10.3
10	2	2	1	83.3	59.9	164.4	17.4	59	7.0	12.6

A target total volume of 20 mL for all tested conditions. The same stock of **5** was used in each experiment, with 25 μL of HPLC samples pipetted from each layer into 5 mL of the diluent.

https://doi.org/10.1021/acs.oprd.1c00118
Org. Process Res. Dev. 2021, 25, 1524−1533

Table 4. Continuous Flow DOE Results for Steps 4−5

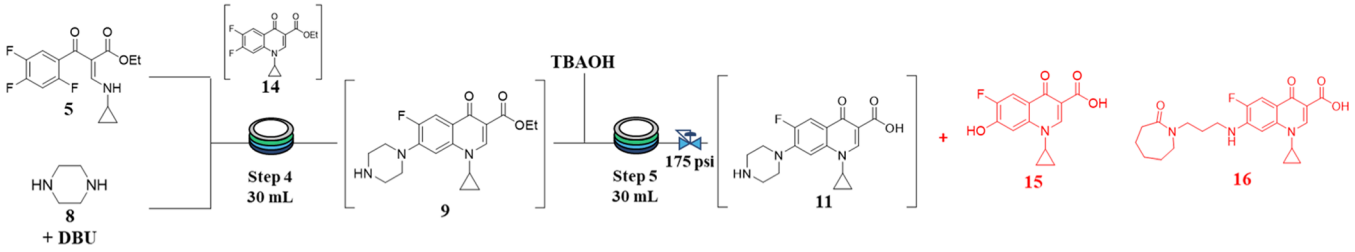

run	step 4 temperature (°C)	step 4 t_g (min)	step 5 temperature (°C)	LCAP of 11 (%)*	11 conc. (mg/mL)*	LCAP of 9 (%)*	LCAP of 15 (%)*	LCAP of 16 (%)*
1	180	5	170	75.9	33.1	0.16	1.6	3.5
2	170	6	160	78.9	33.6	0.22	1.4	3.4
3	160	5	150	79.9	35.6	0.04	0.9	2.9
4	160	5	170	82.2	35.0	0.07	0.9	3.0
5	180	7	170	75.0	33.2	0.47	2.2	4.1
6	160	7	150	78.7	35.3	0.14	1.1	3.3
7	160	7	170	81.6	34.0	0.13	1.1	3.6
8	180	5	150	77.4	34.5	0.33	1.5	3.7
9	170	6	160	79.5	32.0	0.16	1.3	3.7
10	180	7	150	73.9	31.2	1.17	2.1	4.0

The concentration of **5** was held constant at 0.39 M, and the concentrations of **8** and DBU were held constant at 0.9 M (2.6 equiv with respect to **5**). The residence time of step 4 was set by adjusting the inlet flow rates of both the **5** and **8**/DBU feeds. The concentration of TBAOH was held constant at 1.5 M. Equivalents of TBAOH were held constant by adjusting the flow rate. Residence times recorded are V/Q values. * indicates average of duplicate HPLC samples.

Scheme 3. Proposed Side Reaction for the Formation of Impurity Species 16

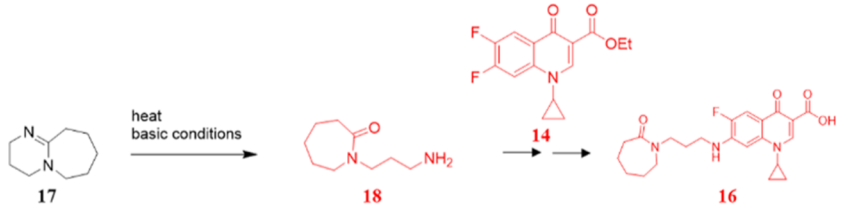

Table 5. Reagent Equivalent Optimization in Continuous Flow for Steps 4−5

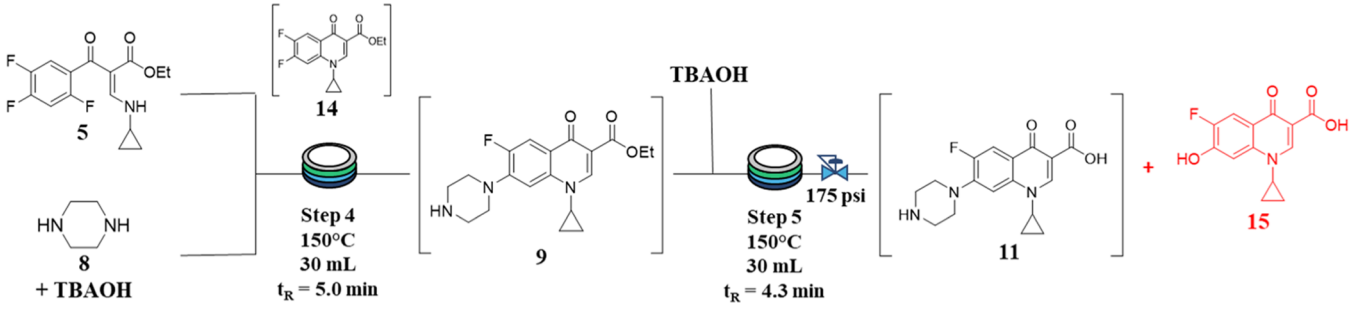

run	8 equiv to 5 (−)	TBAOH equivalents to 5 in step 4 (−)	TBAOH equivalents to 9 in step 5 (−)	LCAP of 11 (%)	11 conc. (mg/mL)	LCAP of 9 (%)	LCAP of 15 (%)
1	3.5	2.5	1.4	84.0	23.2	0.03	8.95
2	3.5	2	1.4	89.0	31.8	0.03	5.47
3	3.5	1.5	1.4	84.9	37.6	10.27	0.78
4	3.5	1	1.4	51.2	21.2	43.31	0.26
5	3.5	1.5	1.97	94.1	31	ND	1.51
6	3.5	1.5	2.14	94.4	31.8	0.02	0.98

The concentration of **5** was held constant at 0.39 M. The flow rates of **5** and **8**/TBAOH were held constant at 2 and 4 mL/min, respectively. The concentration of TBAOH was held constant at 1.5 M. Equivalents of TBAOH in step 4 were controlled by stock preparation. Equivalents of TBAOH into step 5 were controlled via adjusting the flow rate. Residence times recorded are V/Q values.

temperature range studied, and thus, the low set point of 150 °C was selected for future work.

An impurity profile investigation found a species with a molecular weight that aligned with adduct **16** from a plausible

https://doi.org/10.1021/acs.oprd.1c00118
Org. Process Res. Dev. 2021, 25, 1524−1533

Table 6. Continuous Flow Long Runs for Steps 1−3

run	step 1 reactor volume (mL)	step 2 reactor volume (mL)	average LCAP of 5 after step 2 (%)	average conc. of 5 after step 2 (mg/mL)	average LCAP of 5 out of step 3 (%)	average conc. of 5 out of step 3 (mg/mL)	longest continous run duration (h) (τ)	total run duration (h) (τ)
1	10[a]	10[a]		95.3 (s.d. 1.1)	110.1 (s.d. 9.2)	22 (220 τ)	22 (220 τ)	
2	10[a]	5[a]	95.9 (s.d. 0.3)	96.1 (s.d. 18.1)	96.7 (s.d. 0.2)	130.4 (s.d. 1.6)	11 (116 τ)	11 (116 τ)
3	10[a]	5[a]	95.4 (s.d. 0.1)	96.6 (s.d. 1.7)	96.1 (s.d. 0.9)	126.6 (s.d. 11.1)	22 (233 τ)	22 (233 τ)
4	10[a]	5[a]	92.7 (s.d. 4.1)	90.0 (s.d. 4.6)	95.2 (s.d. 0.2)	126.2 (s.d. 2.5)	9 (95 τ)	13 (138 τ)
5	10[a]	5[a]	94.3 (s.d. 0.5)	95.8 (s.d. 1.3)	95.7 (s.d. 0.3)	124.1 (s.d. 6.1)	11 (116 τ)	11 (116 τ)
6	15[b]	7.5[a]	94.9 (s.d. 0.3)	95.2 (s.d. 1.8)	96.1 (s.d. 0.2)	126.4 (s.d. 5.4)	8 (103 τ)	8 (103 τ)

All process parameters were held constant at previously described set points if not shown in the table, with the exception of flow rates, which were scaled linearly with reactor volume to maintain residence time in steps 1 and 2, and extraction ratios in step 3. Reactor dimensions: a = 1/16″ i.d. and b = 0.106″ i.d. Residence times recorded are V/Q values. Run durations additionally denoted in multiples of the combined steps 1−3 residence time as τ.

Table 7. Continuous Flow Long Runs for Steps 4−5

run	step 4 reactor volume (mL)	step 5 reactor volume (mL)	average LCAP of 11 out of step 5 (%)	average conc. of 11 out of step 5 (mg/mL)	longest continuous run duration (h) (τ)	total run duration (h) (τ)	volume of 11 produced (L)	~amount of crude 11 produced (g)
1	60[b]	45[b]	95.1 (s.d. 0.9)	32.8 (s.d 1.7)	8 (58 τ)	32 (234 τ)	21	689
2	60[b]	45[b]	94.3 (s.d. 1.5)	34.6 (s.d 1.7)	8 (58 τ)	8 (58 τ)	7	242
3	60[b]	45[b]	93.5 (s.d. 1.8)	34.2 (s.d 2.9)	9 (65 τ)	26 (190 τ)	18	616
4	60[b]	45[b]	96.1 (s.d. 1.0)	34.1 (s.d 0.6)	10 (73 τ)	10 (73 τ)	8	272
5	60[b]	45[b]	96.6 (s.d. 0.5)	34.2 (s.d 0.9)	9 (65 τ)	12 (88 τ)	9	306
6	60[b]	45[b]	96.6 (s.d. 0.2)	34.3 (s.d 0.4)	10 (73 τ)	10 (73 τ)	8	272

All process parameters were held constant at previously described set points if not shown in the table, with the exception of flow rates, which were scaled linearly with reactor volume to maintain residence time in steps 4 and 5. Reactor dimensions: b = 0.106″ i.d. Residence times recorded are V/Q values. Run durations additionally denoted in multiples of the combined steps 4−5 residence time as τ. All samples taken after step 5.

side reaction involving the hydrolysis of DBU **17** caused by the basic and high-temperature conditions in steps 4−5 (Scheme 3).[24] This impurity species was flagged in the subsequent purification steps as being present at the relatively highest levels and having an extremely low purgability. Therefore, a base screening was performed in batch (see the Supporting Information for details), which revealed that TBAOH was a candidate for the base to be used for step 4 due to a rapid conversion of **5**, with the plausible DBU derivative **16** not being detected. When using TBAOH for step 4 in flow, equivalents of 2.0 and 2.5 with respect to **5** led to increased levels of the hydroxide sensitive impurity species **15** (Table 5; runs 1 and 2). Reducing the equivalents of TBAOH to 1.5 in step 4 led to a purity by LCAP of **11** that exceeded the values previously observed in the DBU process, and an additional charge of TBAOH in step 5 from 1.4 to 1.97 led to the quantitative hydrolysis of **9** (Table 5; run 5).

The chosen process set points for step 4 were 3.5 equiv of piperazine **8** and 1.5 equiv of TBAOH to intermediate **5** at 150 °C for 5 min. The step 5 conditions selected were 1.97 equiv of TBAOH to the theoretical stream concentration of cipro-ester intermediate **9** at 150 °C for 4.3 min. These conditions afford ciprofloxacin **11** with a purity by LCAP of 94 ± 2% and a yield of 90 ± 2% across two reactors with three distinct chemical transformations with an outlet stream concentration of 33 ± 2 mg/mL (Table 5), which fully meets the needs for the material and the production rate and has reduced solubility and clogging concerns.

Process Scale-Up and Continuous Long Runs. Several process intensification efforts around reactor sizing and material throughput were made after initial parameter optimizations. The step 2 reactor was initially minimized from 10 to 5 mL after verifying no significant drop in the LCAP or yield of **5** from the corresponding reduction in residence time. As described above, the hydrolysis (step 5) was observed to be more dependent on equivalents of TBAOH than temperature or residence time, which enabled a residence time reduction to 3.2 min when scaling step 5 without loss in reaction efficacy. Thus, scale-ups were first proposed for step 4 (2-fold in reactor size and volumetric flow rate) and step 5 (2-fold in volumetric flow rate and 1.5-fold in reactor size) as these steps most directly influence the rate of material generation of **11**. Following this, a 1.5-fold scale-up of steps 1−3 with regard to reactor size and volumetric flow rate was proposed in order to expedite the generation of **5** coming out of step 3. The gravity separator volume was held constant as it was observed that the settling and extraction were still effective at the scaled flow rates. To test the consistency and robustness of these scaled-up conditions for future API production scenarios, several continuous end-to-end runs were carried out with a target of either 12 or 24 h duration (Tables 6 and 7). This was performed to ensure that the process and chemistry set points are robust enough to be run longer than the typical experimental length to the steady state and to uncover any necessary process changes or weaknesses to be addressed.

An important aspect of ensuring consistency across runs was ensuring consistent start-up and shut-down procedures. All starting material stocks (except for concentrated TBAOH, which was used as received) for each step were prepared and tested on GC prior to running. For steps 1 and 2, the reactors were first flushed with acetonitrile, and then the reagent lines were primed to the tees by pumping each starting material stock to waste until each respective line contained the starting material. Once primed, the BPR was charged and engaged at the end of the second reactor, followed by beginning reactor heating. Once at the set point temperature, pumping was initiated and the stream was directed to waste for 3−5 residence times before diverting the stream back toward the cross-piece where it was mixed with the aqueous and organic solvents

https://doi.org/10.1021/acs.oprd.1c00118
Org. Process Res. Dev. 2021, 25, 1524−1533

Scheme 4. Finalized Scaled Set Points for the Continuous Ciprofloxacin Synthesis

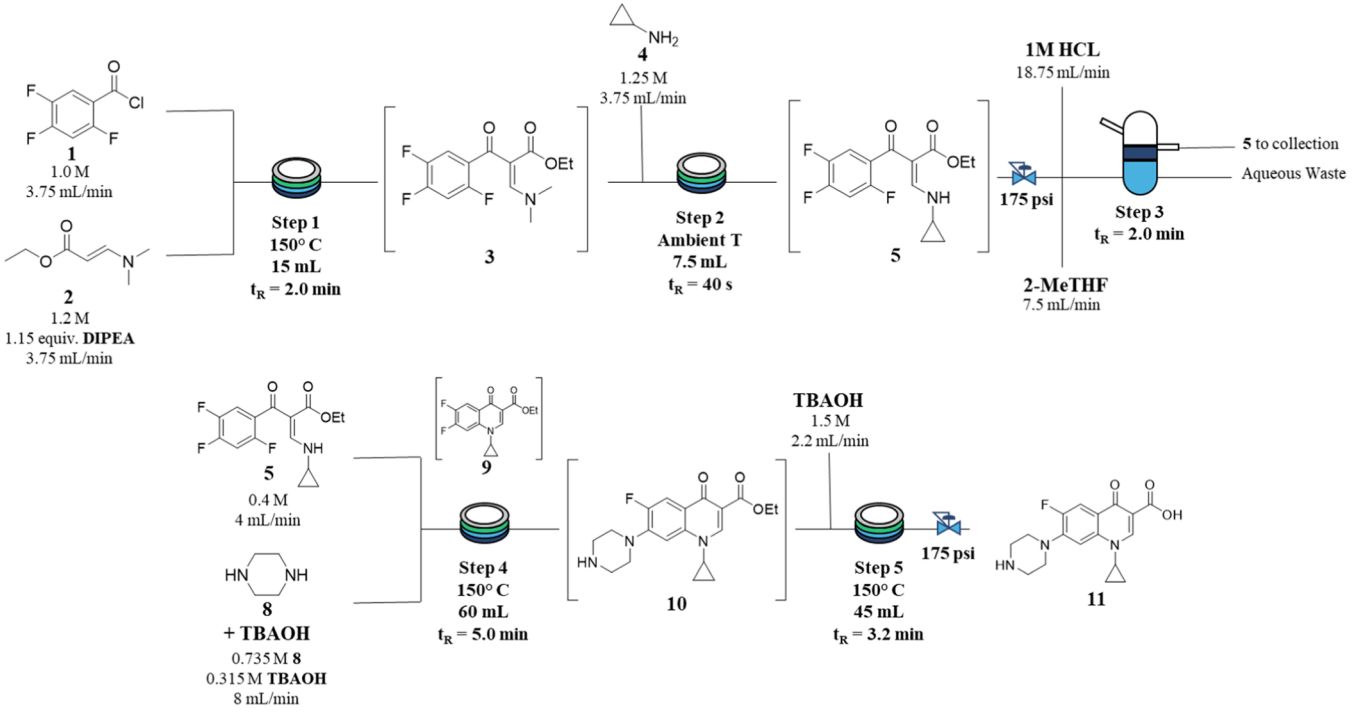

(which had also been primed) for the extraction. The step 3 extraction operation begins filling as soon as the step 2 stream is diverted from waste, and some minor adjustments of the aqueous overflow tee-piece position (see Figure 1b) were initially required to reach a steady equilibrium position that typically does not require further adjustment. The processes are staggered such that steps 4 and 5 are not started until after allowing 20% accumulation (400 mL) in the 2 L surge vessel.

During this accumulation time, a similar start-up procedure takes place for steps 4 and 5, except that these reactors are flushed with dimethyl sulfoxide (DMSO) from the DMSO/piperazine/TBAOH stock line, 2-MeTHF from the step 3 surge vessel line, and water from the TBAOH line. This served to flush the reactors and also prime the reagent lines with their respective solvents, which eased the subsequent priming of the lines. Once primed, the same procedure of BPR engagement, heating reactors to the temperature set point, and then pumping for 3−5 residence times is carried out before beginning collection and sampling of the crude product stream. Shut-down for all steps involved switching from reagent bottles to each line's respective solvent and flushing until the outlet stream was observed to be a colorless solvent, followed by reducing the temperature to ambient conditions while continuing to flush with the solvent. The separator was drained by lowering the aqueous overflow tee-piece and was then taken offline afterward for further cleaning.

Steps 1−3 are consistent with regard to both process equipment stability (capable of running at least 22 h without stoppage) and the reaction stream profile after step 2 and the CLLE in step 3 for intermediate **5**. On occasion, as in run 4 of Table 6, seemingly spurious weaknesses in the reactor fittings occurring over time led to either leaks or chemical releases that required process stoppage. This gradual loss in reactor integrity may also have affected reaction efficacy as run 4 was also observed to have a lower than typical product stream quality relative to the other runs. A routine procedure of changing out fittings and connection tubing ostensibly alleviates this concern and allows for seamless continuous production. This process robustness allows for the rapid generation of intermediate **5** at the desired concentration, purity, and rate of accumulation to be continuously fed into step 4 after staggering the start-up procedures and allowing for approximately 20% volume of the surge vessel after step 3 before beginning the last two steps. Across six runs of durations varying 8−22 h, the purity of **5** out of the step 3 CLLE is observed to consistently meet or exceed 95% purity by HPLC with an average concentration of 126 ± 2 mg/mL.

The long runs for steps 4 and 5 were carried out exclusively with the scaled process conditions to enable the material generation rate of ciprofloxacin **11** required to continuously feed the material into the downstream purification processing operations after staggering start-up procedures. The high-level project goal is continuously manufacturing enough crude ciprofloxacin **11** material to produce 1000 250 mg doses within a 24 h window. The average reaction stream purity range of **11** was 93.5−96.6% by HPLC across six runs, with an average concentration range of 32.8−34.6 mg/mL. At a flow rate of 14.2 mL/min, these runs demonstrate with a high degree of reproducibility the capability of generating the high-quality API material at a rate of ∼29 g/h (∼700 g/24 h) which meets the required production goal assuming continuous production with limited stoppage. This is demonstrated in runs 2, 4, and 6 in Table 7 with net API material generation rates of approximately 30.3 and 27.2 g/h over runs with overall durations of 8−12 h each. Runs 1 and 3 in Table 7 depict attempts at 24 h runs where approximately 616 and 689 g of crude ciprofloxacin **11** were generated in solution over 26 and 32 h, respectively. Processing stoppages (described below) lengthened the material generation time and thus reduced the overall material generation rate.

Several reactor complications with steps 4 and 5 caused the second half of the system to occasionally have to be shut down, flushed, and restarted. The presence of a surge vessel after step 3

https://doi.org/10.1021/acs.oprd.1c00118
Org. Process Res. Dev. 2021, 25, 1524−1533

enabled the continued processing of the first half of the process when this occurred. These issues with steps 4 and 5 typically were related to loosened tubing nuts/ferrules, leaks at the reactor inlet/outlets, or issues with the connection to the BPR and were related to physical aspects of the equipment running under pressure over long time periods. It is hypothesized that transient solids (assumed to be quinolone intermediate **14** or some other insoluble side product) formed over time coating the reactor tubing in step 4 and thus increasing the pressure within the system. With regard to safety concerns of pressure buildup in the system, a pressure relief device (e.g., an additional BPR set to a higher pressure than the BPR maintaining the target system pressure) can be inserted upstream of the reactors using a tee-piece to afford a mechanism for relieving either acute or chronic pressure buildup in the system. The high viscosity of TBAOH and the potential for crystallization in the feed lines was another failure mode identified. This processing risk was handled by way of warming the TBAOH feed bottle to 35 °C and by shortening the length of the lines to and from the TBAOH pump and to the reactor. Without this treatment in the delivery of TBAOH, TBAOH would crystallize in the feed line during start-up, and the line would ultimately have to be flushed with the solvent or replaced and the whole process restarted. Due to these long-duration runs, these concerns were able to be identified and will be addressed to increase the resiliency of future equipment and reactor designs.

The finalized set points for the process are depicted below in Scheme 4 and ultimately yield a product stream out of step 5 that produces ciprofloxacin **11** with a purity by HPLC of 94 ± 2% at a volumetric flow rate of 14.2 mL/min with a concentration of 34 ± 3 mg/mL, which equates to approximately ∼29 g of **11** per hour. Additionally, these set points have been tested in CM scenarios with multiple run durations exceeding 10 h and generating several hundred grams of the crude API material. With regard to the impurity profile, the threshold for tracking impurities was set to 0.1% in the crude product stream and 0.03% in the final API in order to meet the target of less than 0.07% of any impurity in the final API. Impurity species **12** and **13** from the early steps were not observed in the crude product stream above the 0.1% threshold or in the final API above the 0.03% threshold. The unhydrolyzed intermediate species **9** and phenol impurity species **15** were both particularly sensitive to the relative amounts of TBAOH used in steps 4 and 5. Increased TBAOH equivalents led to the nearly complete hydrolysis of **9** (0.0−0.08%) but elevated levels of **15** (0.09−2.0%). This process condition was favored due to the downstream process results from the final API indicating that species **15** had a considerably higher purgability than the unhydrolyzed intermediate **9**. The proposed DBU-related impurity species **16** was not detected in the crude material or the final API during runs following the removal of DBU from the process. Further processing of this material in subsequent purification steps led to purities by HPLC of ciprofloxacin **11** that were >99%. Additionally, the targeting of specific impurities and high purity of the crude reaction stream also allowed for the reduction of impurity levels in the drug product stage to <0.07% by LC. The details of this continuous purification and crystallization process will be detailed in subsequent articles.

CONCLUSIONS

We successfully carried out process development adaptations and set point optimizations and demonstrated reproducibility in long-duration runs for the continuous flow synthesis of the antibiotic ciprofloxacin **11**. The finalized process conditions afforded a yield of 91 ± 2% across the first two steps, giving **5** with a purity of 95 ± 1% by LC, with an extraction efficiency of 88 ± 2% in the CLLE step for **5**. The final two steps afforded a yield of 90 ± 2% with a purity by LC of 94 ± 2%. This was a vast improvement from a process with lower purity values and the formation of the DBU-based impurity **16** with low downstream purgability as well as the tendency to produce solids in-stream and was thus not capable of the run-time required for CM. The first three steps were scaled up 1.5-fold with respect to reactor volume and throughput, and steps 4 and 5 were scaled up 2-fold and 1.5-fold, respectively. This was carried out in order to enable the material throughput required to meet the project's goal of producing enough crude ciprofloxacin **11** material to produce 1000 250 mg tablets within a 24 h window, which was demonstrated with an approximate material production rate of 29 g/h (700 g/24 h). Multiple long runs with durations over 10 h enabled us to identify potential weaknesses in our system as well as ensure confidence in the reproducibility of our set points over the course of CM runs as well as between batches of starting materials and stock solutions. The hundreds of grams of the crude API material generated across these runs were ultimately purified to >99% by continuous crystallization, the process of which is out of the scope of this paper.

ASSOCIATED CONTENT

Supporting Information

The Supporting Information is available free of charge at https://pubs.acs.org/doi/10.1021/acs.oprd.1c00118.

Further descriptions of analytical methods for HPLC, LCMS, and GCMS; additional DOE data and related experimental condition validation data; and plausible impurity molecule characterization (LCMS) data (PDF)

AUTHOR INFORMATION

Corresponding Authors

Luke Rogers − *Department of Chemical Engineering, Massachusetts Institute of Technology, Cambridge, Massachusetts 02139-4307, United States; OnDemand Pharmaceuticals, Rockville, Maryland 20850, United States*; Email: luke@ondemandpharma.com

Tom Roper − *Department of Chemical and Life Science Engineering, Virginia Commonwealth University, Richmond, Virginia 23284-2512, United States*; Email: tdroper@vcu.edu

Authors

Cameron Armstrong − *Department of Chemical and Life Science Engineering, Virginia Commonwealth University, Richmond, Virginia 23284-2512, United States*; orcid.org/0000-0001-6342-0860

Yuma Miyai − *Department of Chemical and Life Science Engineering, Virginia Commonwealth University, Richmond, Virginia 23284-2512, United States*

Anna Formosa − *Department of Chemical and Life Science Engineering, Virginia Commonwealth University, Richmond, Virginia 23284-2512, United States*

Dale Thomas − *Department of Chemical Engineering, Massachusetts Institute of Technology, Cambridge, Massachusetts 02139-4307, United States*

https://doi.org/10.1021/acs.oprd.1c00118
Org. Process Res. Dev. 2021, 25, 1524−1533

Esther Chen − *Department of Chemical Engineering, Massachusetts Institute of Technology, Cambridge, Massachusetts 02139-4307, United States*
Travis Hart − *Department of Chemical Engineering, Massachusetts Institute of Technology, Cambridge, Massachusetts 02139-4307, United States*
Victor Schultz − *Department of Chemical Engineering, Massachusetts Institute of Technology, Cambridge, Massachusetts 02139-4307, United States*
Bimbisar K. Desai − *Department of Chemical and Life Science Engineering, Virginia Commonwealth University, Richmond, Virginia 23284-2512, United States*
Angela Y. Cai − *Department of Chemical Engineering, Massachusetts Institute of Technology, Cambridge, Massachusetts 02139-4307, United States*
Alexandra Almasy − *Department of Chemical and Life Science Engineering, Virginia Commonwealth University, Richmond, Virginia 23284-2512, United States*
Klavs Jensen − *Department of Chemical Engineering, Massachusetts Institute of Technology, Cambridge, Massachusetts 02139-4307, United States*

Complete contact information is available at: https://pubs.acs.org/10.1021/acs.oprd.1c00118

Notes

The authors declare no competing financial interest.

■ ACKNOWLEDGMENTS

The authors would like to acknowledge Gregory Hammersmith, Kersten Rapp, David Brancazio, and Michael Beiro for their engineering support and Steve Cole, Annessa Burnett, and Daniel Cook for their analytical support. This work was supported by the Defense Advanced Research Project Agency (DARPA) under Contract no. HR0011-16-2−0029.

■ REFERENCES

(1) Cole, K. P.; Groh, J. M.; Johnson, M. D.; Burcham, C. L.; Campbell, B. M.; Diseroad, W. D.; Heller, M. R.; Howell, J. R.; Kallman, N. J.; Koenig, T. M.; et al. Kilogram-Scale Prexasertib Monolactate Monohydrate Synthesis under Continuous-Flow CGMP Conditions. *Science* **2017**, *356*, 1144−1150.
(2) Cole, K. P.; Johnson, M. D. Continuous Flow Technology vs. the Batch-by-Batch Approach to Produce Pharmaceutical Compounds. *Expet Rev. Clin. Pharmacol.* **2018**, *11*, 5−13.
(3) Baumann, M.; Moody, T. S.; Smyth, M.; Wharry, S. A Perspective on Continuous Flow Chemistry in the Pharmaceutical Industry. *Org. Process Res. Dev.* **2020**, *24*, 1802−1813.
(4) Lim, J. J.; Arrington, K.; Dunn, A. L.; Leitch, D. C.; Andrews, I.; Curtis, N. R.; Hughes, M. J.; Tray, D. R.; Wade, C. E.; Whiting, M. P.; et al. A Flow Process Built upon a Batch Foundation—Preparation of a Key Amino Alcohol Intermediate via Multistage Continuous Synthesis. *Org. Process Res. Dev.* **2020**, *24*, 1927−1937.
(5) Gutmann, B.; Cantillo, D.; Kappe, C. O. Continuous-Flow Technology - A Tool for the Safe Manufacturing of Active Pharmaceutical Ingredients. *Angew. Chem., Int. Ed.* **2015**, *54*, 6688−6728.
(6) Mascia, S.; Heider, P. L.; Zhang, H.; Lakerveld, R.; Benyahia, B.; Barton, P. I.; Braatz, R. D.; Cooney, C. L.; Evans, J. M. B.; Jamison, T. F.; et al. End-to-End Continuous Manufacturing of Pharmaceuticals: Integrated Synthesis, Purification, and Final Dosage Formation. *Angew. Chem., Int. Ed.* **2013**, *52*, 12359−12363.
(7) Porta, R.; Benaglia, M.; Puglisi, A. Flow Chemistry: Recent Developments in the Synthesis of Pharmaceutical Products. *Org. Process Res. Dev.* **2016**, *20*, 2−25.
(8) Chatterjee, S. FDA Perspective on Continuous Manufacturing. *IFPAC Annual Meeting*; U.S. Food and Drug Administration, 2012.
(9) Moore, C. M. V. Quality by Design-FDA Lessons Learned and Challenges for International Harmonization. *International Conference on Drug Development*; The University of Texas at Austin College of Pharmacy, 2012.
(10) Cole, K. P.; Groh, J. M.; Johnson, M. D.; Burcham, C. L.; Campbell, B. M.; Diseroad, W. D.; Heller, M. R.; Howell, J. R.; Kallman, N. J.; Koenig, T. M.; et al. Supplementary Materials for Kilogram-Scale Prexasertib Monolactate Monohydrate Synthesis under Continuous-Flow CGMP Conditions. *Science* **2017**, *356*, 1144−1150.
(11) On Demand Pharmaceuticals. https://ondemandpharma.com/ (accessed Jun 16, 2020).
(12) Battlefield Pharma. https://themedicinemaker.com/manufacture/battlefield-pharma (accessed Jul 6, 2020).
(13) Adamo, A.; Beingessner, R. L.; Behnam, M.; Chen, J.; Jamison, T. F.; Jensen, K. F.; Monbaliu, J.-C. M.; Myerson, A. S.; Revalor, E. M.; Snead, D. R.; et al. On-Demand Continuous-Flow Production of Pharmaceuticals in a Compact, Reconfigurable System. *Science* **2016**, *352*, 61−67.
(14) Rogers, L.; Briggs, N.; Achermann, R.; Adamo, A.; Azad, M.; Brancazio, D.; Capellades, G.; Hammersmith, G.; Hart, T.; Imbrogno, J.; et al. Continuous Production of Five Active Pharmaceutical Ingredients in Flexible Plug-and-Play Modules: A Demonstration Campaign. *Org. Process Res. Dev.* **2020**, *24*, 2183−2196.
(15) Zhang, P.; Weeranoppanant, N.; Thomas, D. A.; Tahara, K.; Stelzer, T.; Russell, M. G.; O'Mahony, M.; Myerson, A. S.; Lin, H.; Kelly, L. P.; et al. Advanced Continuous Flow Platform for On-Demand Pharmaceutical Manufacturing. *Chem.—Eur. J.* **2018**, *24*, 2776−2784.
(16) WHO. *World Health Organization Model List of Essential Medicines*. Ment. Holist. Heal. Some Int. Perspect., 2019; Vol. *21*, pp 119−134.
(17) Lin, H.; Dai, C.; Jamison, T. F.; Jensen, K. F. A Rapid Total Synthesis of Ciprofloxacin Hydrochloride in Continuous Flow. *Angew. Chem., Int. Ed.* **2017**, *56*, 8870−8873.
(18) Capellades, G.; Neurohr, C.; Briggs, N.; Rapp, K.; Hammersmith, G.; Brancazio, D.; Derksen, B.; Myerson, A. On-Demand Continuous Manufacturing of Ciprofloxacin in Portable Plug-and-Play Factories: Implementation and *In Situ* Control of Downstream Production. *Org. Process Res. Dev.* **2021**, DOI: 10.1021/acs.oprd.1c00117.
(19) Telford, J. K. A Brief Introduction to Design of Experiments. *Johns Hopkins APL Tech. Dig.* **2007**, *27*, 224−232.
(20) SAS Institute Inc. *JMP-8 Design of Experiments Guide*, 2nd ed.; SAS Institute Inc., 2009.
(21) Adamo, A.; Heider, P. L.; Weeranoppanant, N.; Jensen, K. F. Membrane-Based, Liquid−Liquid Separator with Integrated Pressure Control. *Ind. Eng. Chem. Res.* **2013**, *52*, 10802−10808.
(22) Rogers, L.; Jensen, K. F. Continuous Manufacturing − the Green Chemistry Promise? *Green Chem.* **2019**, *21*, 3481−3498.
(23) Hu, D. X.; O'Brien, M.; Ley, S. V. Continuous Multiple Liquid-Liquid Separation: Diazotization of Amino Acids in Flow. *Org. Lett.* **2012**, *14*, 4246−4249.
(24) Hyde, A. M.; Calabria, R.; Arvary, R.; Wang, X.; Klapars, A. Investigating the Underappreciated Hydrolytic Instability of 1,8-Diazabicyclo[5.4.0]Undec-7-Ene and Related Unsaturated Nitrogenous Bases. *Org. Process Res. Dev.* **2019**, *23*, 1860−1871.